Biocatalysis and Biotransformation, January–February 2010; 28(1): 72–82

informa
healthcare

ORIGINAL ARTICLE

Development of a multiphase reaction system for integrated synthesis of isomaltose with a new glucosyltransferase variant

FRANK A. ERHARDT, PHILIP ROSENSTOCK, HENDRIK HELLMUTH & HANS-JOACHIM JÖRDENING

Institute of Technical Chemistry, Section of Technical Biochemistry, Technical University Braunschweig, Braunschweig, Germany

Abstract
A new genetically derived variant of the glucosyltransferase from *Streptococcus oralis* has been characterized physicochemically and kinetically. Compared with the industrially used glucosyltransferase from *Leuconostoc mesenteroides*, the enzyme variant GTF-R S628D possesses 25 times higher affinity for the specific glucosylation of glucose. For a concept of integrated reaction and product isolation, a fluidized bed reactor with *in situ* product removal was applied. The technical feasibility and the applicability of the kinetic models for reaction and adsorption could be demonstrated. The immobilized enzyme was stable (20% activity loss after 192 h) and product could be obtained with 90% purity. A bioprocess model was generated which allowed the integral assessment of the enzymatic synthesis and *in situ* product adsorption. The model is a powerful tool which assists with the localization of optimal process parameters. It was applied for the process evaluation of other glucosyltransferases and demonstrated key characteristics of each enzymatic system.

Keywords: *Glucosyltransferase*, in situ *product removal, modeling, zeolite*

Introduction

Oligosaccharides exhibit great functional diversity and thus are of extraordinary relevance for biological systems (Kannagi et al. 2004; Landsteiner 2004). Apart from their application in medical science (Nilsson et al. 1997; Heerze & Armstrong 2002; Seeberger & Werz 2007), oligosaccharides are used on a large scale in the food industry because of their prebiotic effects and their low glycemic index (Schiweck et al. 1990; Roberfroid 2007). Isomalto-oligosaccharides are a mixture of di- to hexasaccharides (Buchholz & Seibel 2003). In 2004, the annual isomalto-oligosaccharide output amounted to 11 000 tons (Taniguchi 2004). However, selective synthesis of a single isomalto-oligosaccharide like the disaccharide isomaltose is difficult.

Generally, three approaches to oligosaccharide formation can be distinguished: hydrolysis of polymers, reverse hydrolysis of monosaccharides in solutions with low water activity and transglycosylation in aqueous solutions (Monsan & Paul 1995; Hansson & Adlercreutz 2001). The first approach lacks sustainability and is often not cost-effective due to the high cost of substrates (dextranase–dextran system; e.g. Mountzouris et al. 2002). The required endo-glycosidases also yield a broad product spectrum with varying degrees of polymerization (*DP*) instead of a single pure compound. However glycosidases can facilitate oligosaccharide synthesis by reverse hydrolysis. Using activated donors, high molar yield coefficients can be obtained under mild reaction conditions (e.g. 60% for isomaltose; Vetere et al. 2000), although reverse hydrolysis is not regioselective and is an equilibrium-controlled reaction. Thus, high amounts of substrate and activated donor remain in the product solution and result in low product purity.

Transglycosylation reactions are catalyzed by the enzyme family of glycosyltransferases (GTFs); in the case of Leloir GTFs with a requirement for activated substrates. For example, dextransucrase (DSR-S) converts the inexpensive substrate sucrose into dextran at technical scale (Naessens et al. 2005). GTFs like DSR-S transfer the glucosyl moiety from sucrose

Correspondence: H.-J. Jördening, Institute of Technical Chemistry, Section of Technical Biochemistry, Technical University Braunschweig, Hans-Sommer-Straße 10, D-38106 Braunschweig, Germany. Tel: +49-531-391 7261. Fax: +49-531-391 7263. E-mail: A.Joerdening@tu-bs.de

ISSN 1024-2422 print/ISSN 1029-2446 online
DOI: 10.3109/10242420903474866

highly selectively to a growing polymer chain with $DP=i$ via an α-1,6 glycosidic linkage with displacement of fructose (equation (1)). In general, the reactions are regio- and stereoselective, and proceed even at low concentrations in water with high yield.

$$n\ \text{sucrose} + (1,6\text{-}\alpha\text{-D-glucosyl-})_i \xrightarrow{\text{DSR-S}} (1,6\text{-}\alpha\text{-D-glucosyl-})_{i+n} + n\ \text{fructose} \quad (1)$$

Alternatively glucose can be transferred to an external acceptor like glucose to form isomalto-oligosaccharides (equation (2)). The yield of product depends on both acceptor quality (Robyt & Eklund 1983) and quantity (Berensmeier et al. 2006). The degree of sucrose hydrolysis is usually low as water is a weak acceptor. Glucose, isomaltose or isomaltotriose act as strong acceptors. Thus, follow-up reactions take place and a homologous series of oligosaccharides is generated (Pereira et al. 1998; Tanriseven & Dogan 2002).

$$\text{sucrose} + \text{glucose} \xrightarrow[\text{-fru}]{\text{DSR-S}} \text{isomaltose} + \text{glucose} \xrightarrow[\text{+suc; -fru}]{\text{DSR-S}} \text{isomaltotriose}\ldots \quad (2)$$

The approach using GTFs overcomes some limitations of using enzymes that need activated sugars (e.g. UDP-Glucose) as substrate (cost-effective substrate, water as solvent, high conversions, thus no substrate remaining in product solution). However the product purity still suffers from impurities like high amounts of acceptor (500 g L^{-1}; Ergezinger et al. 2006) and follow-up products. It is thus imperative to further increase the selectivity of the biocatalyst and also to tailor the product spectrum. The latter could be realized by *in situ* product removal (ISPR) which suppresses follow-up reactions. Ergezinger et al. (2006) increased the overall product yield (isomaltose) by up to 25% using ISPR in a fluidized bed reactor (FBR).

Regarding the improvement of biocatalyst selectivity, recent studies have focused on the implementation of endo-dextranase in the DSR-S reaction system, either in soluble form in an enzyme membrane reactor (Kim & Day 1994; Goulas et al. 2004; Kubik et al. 2004) or co-immobilized in alginate beads (Erhardt et al. 2008a,b). However, the instability of DSR-S in the presence of excess dextranase hinders the technical application.

The current study aimed to develop an enzymatic process for isomaltose synthesis with ISPR. From previous engineering and screening studies a new enzyme variant GTF-R S628D (E.C.2.4.1.5) was obtained (Hellmuth et al. 2008) showing increased hydrolysis (11%), but most notably increased formation of small acceptor products (89%). No dextran formation occurs. This variant bears a single mutation near the putative transition-state stabilizer D627. In different glucansucrases, mutations in this region showed structural changes of the polymer formed (Kralj et al. 2005; Moulis et al. 2006). Possibly nucleophilic attack as well as the release of acceptor products are facilitated due to this mutation, but because a three-dimensional structure for this type of enzyme has been published only recently (Pijning et al. 2008), precise explanations are lacking.

Materials and methods

Enzyme production

Fermentation and cell disruption. The gene encoding GTF-R S628D was available on the recombinant plasmid pTH275 hosted in *Escherichia coli* XL10-gold (Hellmuth et al. 2008). Shaken flask cultures were routinely grown at 27°C on LB medium (tryptone 10 g L^{-1}, yeast extract 5 g L^{-1}, NaCl 10 g L^{-1}) supplemented with ampicillin 0.1 g L^{-1}. For large-scale growth, starter cultures (cell dry weight (CDW) 2.5 g L^{-1}) were inoculated (5% v/v) into 50 L defined medium which consisted of (g L^{-1}): glucose (20), KH_2PO_4 (13.3), $(NH_4)_2HPO_4$ (4), citric acid (1.7), $MgSO_4$ (1.2), Fe(III) citrate (0.1), ampicillin (0.1), thiamin (4.5×10^{-3}) and trace elements ($CoCl_2$ (10 μM), $MnCl_2$ (75), $CuCl_2$ (9), H_3BO_4 (48), Na_2MoO_4 (9), Fe(III) citrate (400)), pH 6.5 Bacteria were grown at 30°C with a gassing rate of 0.5 v/v per min at 460 rpm. After 17 h, cell suspension (CDW 4.1 g L^{-1}) was harvested by centrifugation at 11 000*g* for 25 min at 10°C. Cell washing and re-suspension were performed in 25 mM sodium acetate buffer, pH 5.4. For cell breakage, biomass was subjected to ultrasonication (200 W; 7 MJ kg-biomass^{-1}).

Fermentation was done without induction and yielded GTF-R enzyme activity of 90 U L^{-1}.

Enzyme purification and immobilization. Enzyme immobilization required the formation of a protein–dextran complex. Dextran formation was achieved by enzymatic conversion of sucrose 10 g L^{-1} at 30°C. For enzyme immobilization, 1 L enzyme solution with an activity of 3.3 U mL^{-1} was prepared for application in a FBR according to Berensmeier et al. (2004). About 1.3 kg in Ca-alginate-immobilized biocatalyst with a particle diameter of 0.5 mm and an activity of 1.2 U g^{-1} (70% yield) could be obtained using a jet cutter (GeniaLab Ltd, Braunschweig, Germany).

In Table I, a qualitative comparison with two other enzymatic systems shows that GTF-R had the highest potential for isomaltose formation. It needed

Table I. Comparison of GFT-R with two other enzyme systems with respect to isomaltose formation.

Enzyme	K_Y (mol mol^{-1})	Y_{max} (mol%)
GFT-R	0.8	60
DSR-S + dextranase	4.3	60
DSR-S	18.3	60

a glucose/sucrose ratio (K_Y) of less than one, giving an isomaltose yield on sucrose (Y_{max}) at the same level as both of the other systems with much higher glucose/sucrose ratios.

Storage stability and activity studies at different temperatures and pH values

To compute half-lives of the immobilized enzyme a first-order decay model was applied. Different buffer systems were investigated at 35°C in 25 mM $CaCl_2$ in 25 mM buffer (4.6≤pH≤5.2, benzoic acid; 5.2≤pH≤5.8, sodium acetate; 5.8≤pH≤7.0, imidazole). Activity assays were performed in 25 mM $CaCl_2$ in 25 mM buffer (3.5≤pH≤5.0, sodium acetate; 5.0≤pH≤6.4, piperazine; 6.4≤pH≤8.0, imidazole; 8.0≤pH≤8.5, glycine). At pH 5.8, Bis-Tris (bis(2-hydroxyethyl)amino-tris (hydroxymethyl)methane), MES (2-(4-morpholino) ethanesulfonic acid), imidazole, benzoic acid and sodium acetate were used as buffer systems to determine storage stability.

Reaction conditions for kinetic experiments and in situ *product removal*

The GTF-R S628D immobilizate (7.5 g) was incubated in 25 mL reaction solution (0.1–1 M sucrose and 0–2 M glucose in 25 mM calcium acetate buffer at pH 5.8) at 30°C in a shaking water bath. For the semi-technical scale bioconversion, 1.2 kg immobilized GTF-R S628D were incubated in a FBR with ISPR (234 mM sucrose and 560 mM glucose; 0.15 U mL^{-1}; 30°C; pH 5.8). As selective adsorbent β-zeolites with Si/Al ratio of 75 were applied (Süd-Chemie Ltd, Munich, Germany) at a solid phase concentration of 100 g L^{-1}. Adsorption properties of zeolites for mono- and disaccharides have been reviewed by Berensmeier & Buchholz (2004). The reactor was operated quasi-continuously. A process flow sheet of the FBR and its operation are described in the 'Fluidized bed reactor' section below.

Modeling

Kinetic modeling of product formation. Parameters for the kinetic model were obtained from experiments with GTF-R S628D under various sucrose/glucose conditions. We adopted a previously developed GTF model for the acceptor reaction (Heincke et al. 1999). The significance of model parameters could be demonstrated by sensitivity analysis and the model has also been verified for other GTFs (Dols et al. 1999). Equation (3) describes the substrate consumption neglecting substrate inhibition, which was not observed for this enzyme variant.

$$\frac{\mathrm{d}suc}{\mathrm{d}t} = -\frac{E_0 \cdot suc \cdot (p_1 + p_2 \cdot glc)}{1 + p_3 \cdot suc + p_4 \cdot glc + p_5 \cdot glc \cdot suc + p_6 \cdot glc^2} \tag{3}$$

suc and *glc* are the sucrose and glucose concentration. Parameter p_3 was set to the reciprocal of the Michaelis–Menten concentration, enzyme activity E_0 could be taken from experimental conditions and parameter p_4 could be computed from parameters p_1, p_2 and p_6 (Heincke et al. 1999). Thus, four parameters were ascertained by non-linear regression using a training set of initial rates at different experimental conditions by the Levenberg–Marquardt algorithm (see Figure 2). A table with the actual parameter data is given in the Appendix. Using equation (3), sucrose conversion can be simulated.

Likewise, isomaltose concentration (*im*) can be modeled taking account of the molar yield coefficient $Y_{im/suc}$ (equation (4)). The calculation of $Y_{im/suc}$ is described in more detail in the 'Results and discussion' section (equation (9)) and must also consider sucrose hydrolysis ($Y_{H2O/suc}$=0.1; experimental data).

$$\frac{\mathrm{d}im}{\mathrm{d}t} = -\frac{\mathrm{d}suc}{\mathrm{d}t} \cdot Y_{im/suc} \tag{4}$$

Modeling of integrated adsorption on β-zeolite and synthesis. Adsorption is expressed as a kinetic term in which the change in covered places of the adsorbent (*cp*) is calculated by adsorption (rate constant ads_{k1}) of solute isomaltose onto free places (*fp*). Desorption is considered by the rate constant ads_{k-1} (equation (5)). As equilibrium is rapid, no adsorption kinetics could be determined; the ratio of ads_{k-1} over ads_{k1} represents the dissociation constant. This constant is equal to the quotient of saturation capacity over the adsorption equilibrium constant (Berensmeier & Buchholz 2004; Ergezinger 2006). As a further boundary condition, the number of free adsorption sites *fp* is limited (zeolite concentration times the saturation capacity).

$$\frac{\mathrm{d}cp}{\mathrm{d}t} = ads_{k1} \cdot im \cdot fp - ads_{k-1} \cdot cp \tag{5}$$

Equation (4) is cast into equation (6) to model continuous operation with a residence time τ. Adsorption,

desorption and export of loaded zeolite are also included.

$$\frac{\mathrm{d}im}{\mathrm{d}t} = -\frac{\mathrm{d}suc}{\mathrm{d}t}\cdot Y_{im/suc} + \left(im_{t0} - im_t\right)\cdot\frac{1}{\tau} - ads_{k1}\cdot im\cdot fp + ads_{k-1}\cdot cp - \frac{cp}{\tau} \qquad (6)$$

Modeling of specific zeolite loads for various reaction conditions and enzymes. In contrast to sucrose, glucose competes with isomaltose for free places on the zeolite. A glucose-dependent adsorption equilibrium parameter K_d can be calculated via equation (7). The parameter decreases exponentially and half of initial K_d is attained at 880 mM glucose.

$$K_\mathrm{d} = ads_0 + ads_1\cdot\exp\left(-\frac{glc}{ads_2}\right) \qquad (7)$$

The molar yield coefficient $Y_{im/suc}$ can be computed for any glucose/sucrose ratio. Multiplied by the initial sucrose concentration the yield coefficient gives the overall product concentration. By use of a mass balance the specific load of β-zeolite with adsorbed isomaltose can be computed from the overall and equilibrium isomaltose concentration. The iterative calculation of specific load was performed with Microsoft Excel® using the solver function and macros.

Modeling of process efficiency. In order to assess the overall process efficiency under defined process conditions (i.e. sucrose/glucose concentration, enzymatic system), equation (8) was applied. The amount of adsorbed isomaltose on the zeolite ($q*$) was computed as discussed in the preceding section on 'Modeling of specific zeolite loads'. Reaction rate r_max depends on sucrose and glucose concentration in the reaction mixture and can be calculated according to equation (3). As a boundary condition, sucrose conversion was considered from the initial sucrose concentration (c_{suc}) until $c_{suc,10\mathrm{mM}}$ = 10 mM remaining substrate (i.e. K_M of enzyme). The first term of equation (8) reflects the equilibrium load of zeolite, and this is related to the reaction time which is necessary for sucrose conversion (second term). The third term takes account of the surface coverage of the adsorbent ($q*$ over q_max); from a practical point of view, downstream processing (DSP) of highly loaded zeolites is preferred to DSP of marginally loaded carriers. Thus, efficiency is optimal when zeolites are almost fully loaded at reaction times as short as possible.

$$\text{Efficiency} = q^*\cdot\frac{r_\mathrm{max}}{c_{suc,\mathrm{ini}} - c_{suc,10\,\mathrm{mM}}}\cdot\frac{q^*}{q_\mathrm{max}} \qquad (8)$$

Assessment of isomaltose bound on zeolite

Suspension from the multiphase reactor was centrifuged at 5200*g* for 20 min (30 mL in Falcon tubes). Supernatant (10 mL) was withdrawn for HPLC analysis and 5 mL EtOH was added for desorption. Quantitative desorption measured by HPLC occurred at 70°C over a period of 5 days. To gravimetrically measure the zeolite mass, the desorbed suspension was washed three times with dH_2O, dried at 70°C and desiccated. Following this procedure the specific load (isomaltose per weight zeolite) could be computed. Mass balances indicate that desorption was quantitative under the conditions given above.

Downstream processing of zeolites from the fluidized bed reactor. After solid/liquid separation in a dead-end filtration unit (black ribbon filter, pore size <5 μm) one aliquot of zeolite was immediately desorbed with ethanol (200 g L^{-1} zeolite suspension; 50% v/v EtOH; 70°C; 5 days). The remaining zeolites were re-suspended in dH_2O (50°C; 200 g L^{-1} zeolite suspension; 4 mL water/g zeolite), stirred for 1 h and filtered/desorbed as described above. If necessary, the procedure was repeated. Purities were calculated on a w/v basis and yields of processed zeolites were benchmarked against the immediately desorbed zeolite aliquot. Detailed information is given in Holtkamp et al. (2009).

Enzyme activity assay (dinitrosalicylic acid test)

One unit of GTF activity refers to the amount of enzyme that liberates 1 μmole of fructose per minute at pH 5.8 and 30°C using sucrose 100 g L^{-1} in 25 mM calcium acetate buffer. Reducing sugars were measured with dinitrosalicylic acid (DNS) solution according to the protocol of Sumner & Howell (1935). Linear regression of the fructose formation over a 2 h time period was used for final computation of GTF activity. Investigation of the effect of metals upon GTF-R activity showed that the presence of 10 mM heavy metals significantly distorted the slope of the calibration line (water, 100%; Cu^{2+}, 65%; Ni^{2+}, 130%; Zn^{2+}, Co^{2+}, 180%; EDTA, Mn^{2+}, 230%).

Fluidized bed reactor

A process flow sheet for the GTF-R bioreactor is presented in Figure 1. An eccentric pump generated the fluidization of biocatalyst in the FBR. Mesh sizes

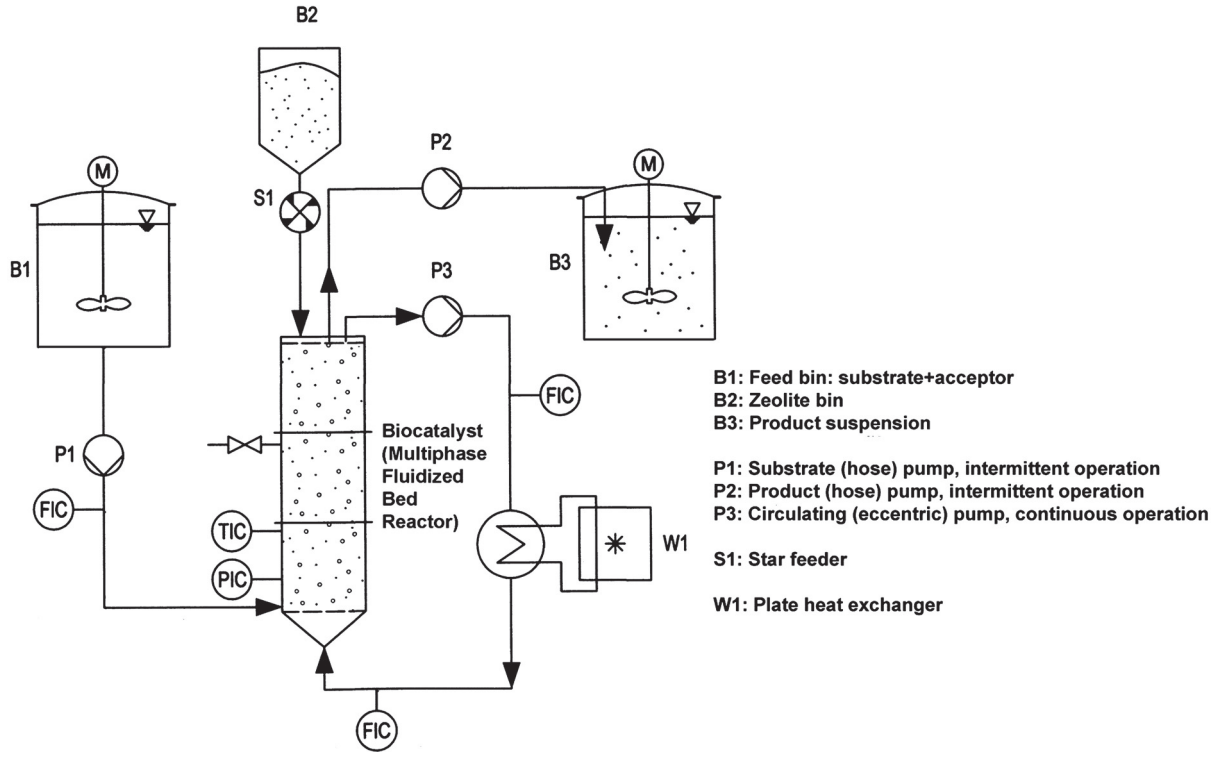

Figure 1. Process flow sheet for the fluidized bed reactor (reactor height = 2 m; reactor diameter = 0.1 m; flow rate = 0–1 L h^{-1}; temperature = 30°C).

of the sieves at the bottom and top of the reactor were adapted to the particle size of the adsorbent phase (zeolite; particle diameter = 10–60 μm). By doing so, this could freely circulate in the fluid phase while the biocatalyst (diameter 0.5–1 mm) was retained in the reactor. Sucrose and glucose were fed quasi-continuously from a feed bin. Because the β-zeolite undergoes aging in aqueous solution, it must be separately added to the reactor as a dry powder. Product suspension with zeolite was withdrawn and after sieve box centrifugation the loaded adsorbent was further processed. DSP involved washing of the zeolite and desorption with 50% v/v ethanol. After zeolite reconditioning it could be recycled. Ergezinger et al. (2006) reported on a continuous approach for DSP of adsorbent with recirculation of material fluxes (reaction supernatant, washing and stripping agents), so in principle the overall process could be operated in a continuous manner.

Quantification of intermediates by HPLC

Carbohydrate concentrations were quantified using external standards with a refractive index detector (30°C). Samples were separated by HPLC with an amino-bonded stationary phase analytical column (Purospher Star NH_2 5 μm, 250 mm × 4.6 mm i.d.; Merck, Darmstadt, Germany) with acetonitrile–water (80% v/v) as mobile phase at a linear velocity of 1 mm s^{-1}. To remove zeolites and dust from reaction solutions, samples were centrifuged and subjected to membrane filtration (0.2 μm, nitrocellulose; Millipore, Schwalbach, Germany). Samples were diluted so that the total sugar concentration did not exceed 50 g L^{-1}.

Results and discussion

Characterization of GTF-R S628D

Enzyme activity and stability under various physicochemical conditions. Regarding enzyme activation by 10 mM calcium ions (Berensmeier 2003; Ergezinger 2006), complete activity loss in the presence of 10 mM zinc and copper (Miller & Robyt 1986; Berensmeier 2003) and the pH-dependent activity profile (maximum activity at pH 6.5, 80% activity within pH 4.8–7.2; Tuomanen et al. 2000), results from the enzyme variant correspond well with the properties of the wild-type enzyme. However, the enzyme variant exhibited maximal activity at a temperature of 42°C which was higher than that of DSR-S (34°C; Monchois et al. 1998) and the GTF-R wild-type (38°C; Berensmeier 2003). Activation energy was computed using the Arrhenius equation, giving E_A = 33±3 kJ mol^{-1}.

Inactivation occurred at temperatures above 45°C (E_{IA} = 270±60 kJ mol^{-1}).

To locate optimal stability parameters for long-term biocatalysis, storage stability studies of the immobilized enzyme were carried out.

The half-life of GTF-R S628D dropped sharply from 37 h at 35°C to only 4.1 h at 40°C, so the operating temperature should be well below 35°C (37 h). At a temperature of 30°C, the half-life ($t_{1/2}$) of immobilized enzyme under process conditions (0.6 M glucose, 0.2 M sucrose) was 22 days and surpassed the extrapolated $t_{1/2}$ from stability studies (9 days at 30°C). Furthermore, the energy of inactivation for $t_{1/2}$ compares very well with that of DSR-S (323±7 kJ mol^{-1} rather than 353 kJ mol^{-1}; Berensmeier et al. 2006). In studies of operating pH, the highest half-life was achieved at pH 5.8 ($t_{1/2}$ = 37 h compared with $t_{1/2}$ = 21 h at pH 7 and $t_{1/2}$ = 1.9 h at pH 4.6) and different buffer systems for this pH value were evaluated. Bis-Tris, sodium acetate, MES and imidazole (25 mM buffer in 25 mM calcium chloride) did not affect biocatalyst stability. Benzoic acid also has antimicrobial potential, but decreased $t_{1/2}$ by 70% (data not shown). A negative effect of benzoic acid (90% decrease of GTF activity with 1 mM benzoic acid) has also been reported by Taguchi et al. (1997).

Characterization of reaction kinetics. Kinetic constants of native and (used) immobilized biocatalyst were determined. Compared to the GTF-R wild-type (0.9 mM; Berensmeier 2003), K_M differed significantly (3.8 mM). Enzyme entrapment resulted in a further change of the apparent K_M of GTF-R S628D. Diffusional limitations caused an increase in K_M by a factor of 2.5 (to 9.6 mM sucrose) at a specific activity of 1.34 U g-beads^{-1}. A shift in specific activity and K_M after operation in the FBR (specific activity = 1.06 U g^{-1}; K_M = 8.1 mM) might point at a slow, abrasive disintegration of the alginate matrix.

Figure 2 presents experimental and modeled data of initial reaction rates at various sucrose and glucose concentrations. Apparently glucose acts as an effector up to 1 M and increases reaction rate up to 300%. Competitive inhibition takes place at higher glucose concentrations and has to be taken into account in the model (parameters p_6 (p_2, p_4) in equation (3)). The comparatively low positive effect of sucrose at moderate and high glucose concentrations is also considered by parameter p_5. Substrate inhibition has been reported for DSR-S (Berensmeier et al. 2006), but not for the GTF-R wild-type (Berensmeier 2003), while GTF activity can be accelerated or slowed down by glucose (Koepsell et al. 1953; Berensmeier et al. 2006).

Because glucose serves as an acceptor, high concentrations will cause high yields of acceptor product

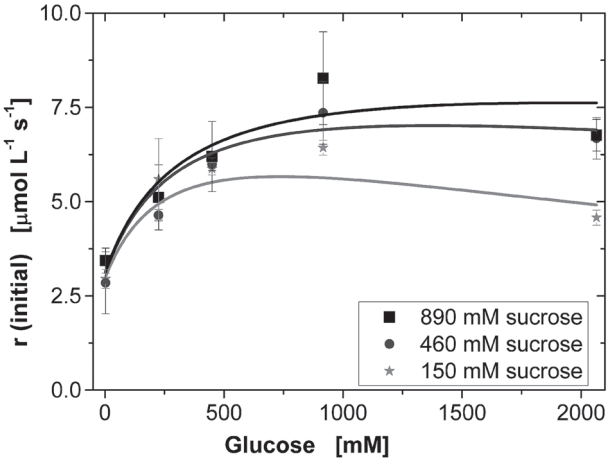

Figure 2. Initial reaction rates of G TF-R S628D at different sucrose/glucose concentrations (solid lines, kinetic model).

(Figure 3). Molar yield coefficients of isomaltose can be modeled reasonably well for a broad spectrum of experimental conditions using a saturation model (equation (9)). In this model K_Y displays the acceptor/substrate ratio at which half-maximal yield is obtained. Thus it is an affinity measure for glucosyl transfer (K_Y = 0.8 mol mol^{-1}).

$$Y = \frac{Y_{max}}{1 + K_Y \cdot glc \cdot suc^{-1}} \qquad (9)$$

The affinity for glucosyl transfer by GTF-R S628D surpasses that of DSR-S by a factor of 25 and that of DSR-S co-immobilized with dextranase by a factor of 5 (Berensmeier et al. 2006; Erhardt et al. 2008a). However, the formation of α-1,6 glycosidic linkages

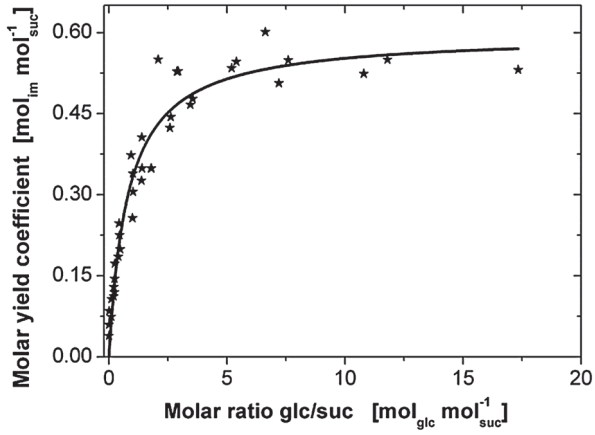

Figure 3. Molar yield coefficient of isomaltose formation at different molar ratios of acceptor and substrate (volumetric enzyme activity = 0.05–0.5 U mL^{-1}; sucrose concentration = 0.1–1 M; glucose concentration = 0–2 M; solid line, saturation model; Y_{max} = (0.60±0.02) mol-im mol-suc^{-1} ; K_Y = (0.80 ± 0.09) mol-glc mol-suc^{-1}).

by the GTF-R variant is slightly less selective compared with the DSR-S enzyme ($Y_{max,GTF\text{-}R\ S628D} = 0.60$; $Y_{max,DSR\text{-}S} = 0.69$; Erhardt et al. 2008a). A successful integrated production strategy requires a biocatalyst with low K_Y value, because glucose concentration must remain as low as possible in the process. This is not only due to problems of glucose in downstream processing (co-adsorbed, void volume; Ergezinger 2006), but also due to the lower selectivity for production of isomaltose (equation (7); Berensmeier & Buchholz 2004).

Using equations (3) and (4), kinetics of substrate conversion and product formation can be modeled. This basic model considers the release of glucose from sucrose hydrolysis and its removal for acceptor reaction/isomaltose synthesis (sucrose 168 mM and 985 mM, glucose 0 mM; Figure 4). Other by-products of transglucosylation are not considered, since they could not be detected (polymer retention in the alginate matrix) or are produced only at very high sucrose conversions (leucrose, isomaltulose). Isomaltose concentration is simulated well at different glucose/sucrose ratios via the computed yield coefficient (equations (4) and (9); remaining kinetics in Figure 4). Particularly at high molar saccharide concentrations the sucrose concentration profiles were difficult to predict, which might suggest external transport limitations. Although GTFs exhibit multiple molecular interactions (Dols et al. 1999; Heincke et al. 1999; Ergezinger 2006), the kinetic model produces reasonable data with a low number of parameters. Next, modeling should integrate the *in situ* adsorption step.

Production and isolation of isomaltose using a continuously operated fluidized bed reactor with in situ product removal

The FBR with ISPR is used to produce isomaltose in a continuous manner on a semi-technical scale (Figure 5). Residence times were 20 h, 40 h and infinity (batch mode). The modeled concentration courses of substrate and product are well represented which is also in agreement with modeling data from

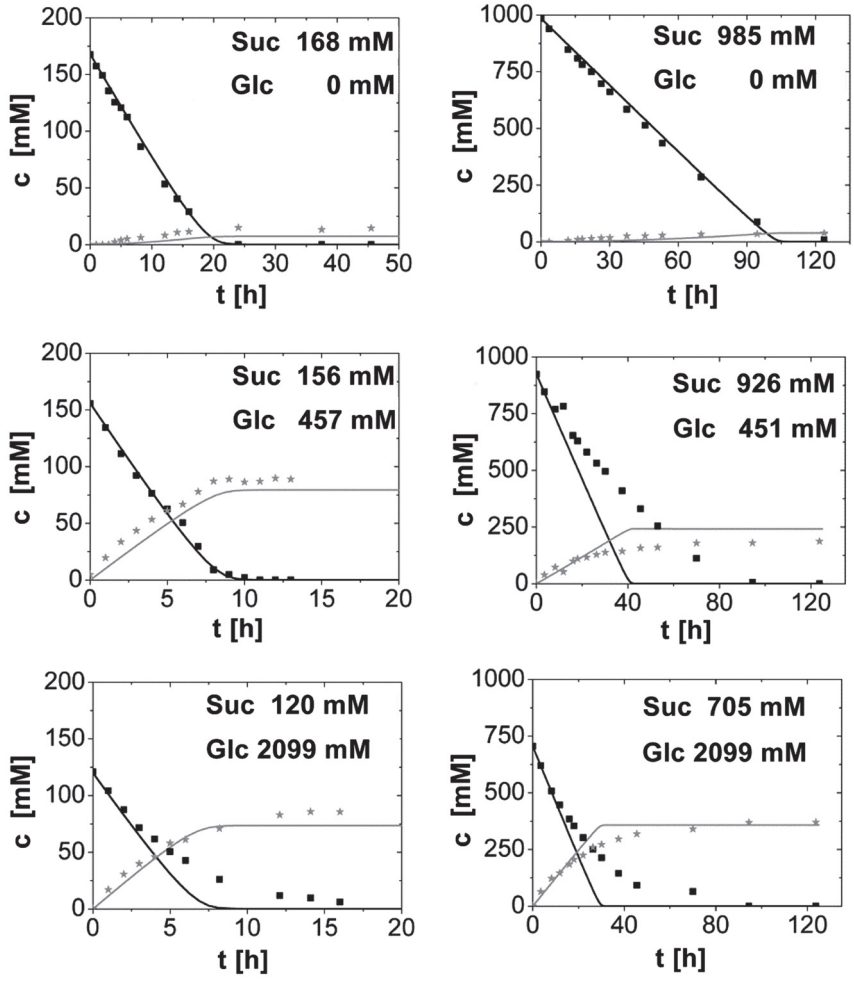

Figure 4. Comparison of experimental and modeled kinetics of immobilized GTF-R S628D (■, sucrose data; ★, isomaltose data).

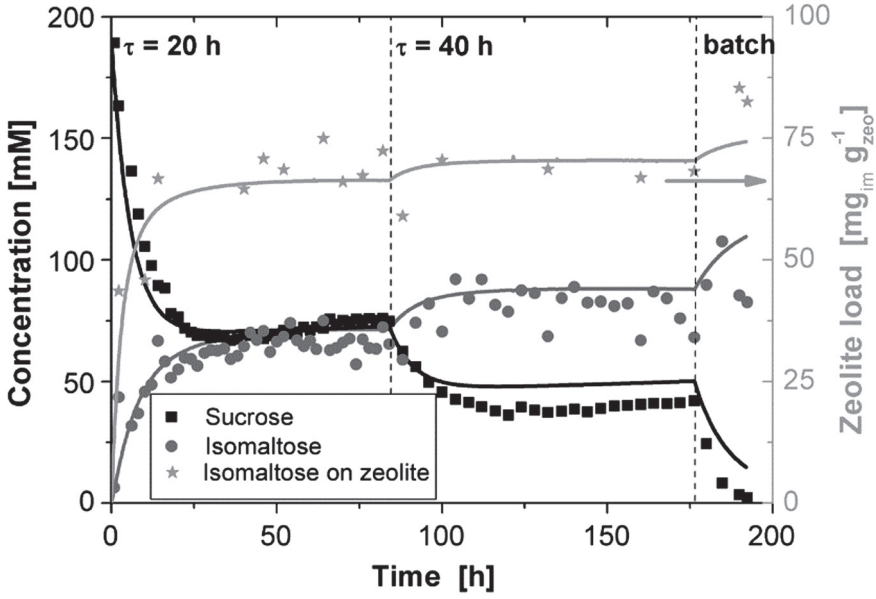

Figure 5. Product formation in the continuous fluidized bed reactor using 560 mM glucose, 234 mM sucrose and β-zeolite 100 g L^{-1} (reaction volume = 15 L; enzyme activity = 0.15 U mL^{-1}; pH 5.8; 30°C; solid lines, kinetic model).

Figure 4 (see plot with 156 mM sucrose/457 mM glucose).

Incorporation of a kinetic adsorption model (equations (5) and (6)) results in good agreement between actual and simulated data for isomaltose in the fluid and on the solid phase. However, quantification of zeolite-bound isomaltose is challenging, although a previous protocol (Ergezinger et al. 2006) could be improved. Quantitative desorption demands harsh conditions (desorption at 70°C in 50% v/v ethanol for 5 days) and the minor changes in concentration make analysis difficult. Figure 5 indicates that even the doubling of isomaltose concentration during reaction results in only a slight increase in zeolite-bound isomaltose. This is due to the reduced selectivity of zeolite (equation (7)) even at moderate glucose concentrations. After 192 h of operation, the reaction mixture consisted of 65% glucose, 19% fructose, 4% fructose acceptor product (leucrose) and 12% isomaltose (4% adsorbed on solid phase, 8% in fluid phase).

When the zeolite was immediately desorbed after solid/liquid separation, the purity of isomaltose could be tripled from ~10% in the reaction supernatant to greater than 30% in the desorption solution (Figure 6). Initial purity surpassed that of a process using DSR-S with glucose 500 g L^{-1} by a factor of 3 (Ergezinger et al. 2006). The yield for 60% pure isomaltose is also three times higher for the GTF-R variant (60% yield) compared with DSR-S (20% yield). In both cases isomaltose could be further purified up to 90% purity (20% yields). When zeolite is washed with water, it predominantly removes adsorbent-associated contaminants, but also some isomaltose. Product loss during aqueous washing steps does not seem to be typical of processes with ISPR (Hilker et al. 2004; Jördening et al. 2008). However, in many cases the compound of interest is hydrophobic and adsorbed on an organic polymer. In this respect the polar isomaltose, which is adsorbed on an inorganic carrier, differs significantly. Furthermore, 100% pure isomaltose cannot be expected even after extensive washing, because water only removes contaminants of the void volume and not of co-adsorbed compounds. Although the DSP itself could be further optimized via fine-tuning

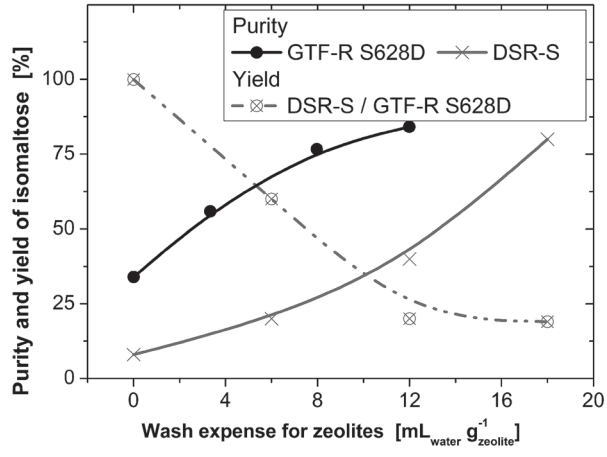

Figure 6. Effect of zeolite washing upon product quality (DSR-S data from (Ergezinger 2006); product suspension obtained from different reaction solutions: DSR-S = 2.77 M-glc; GTF-R S628D = 0.56 M-glc).

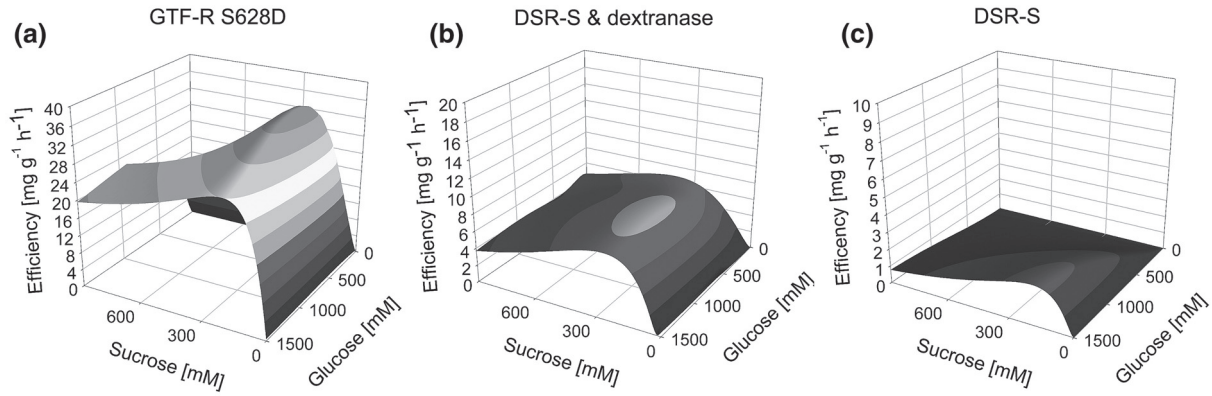

Figure 7. Process efficiency for different enzymatic systems (β-zeolite = 200 g L^{-1}; activity = 8.5 U-GTF mL^{-1}): (a) GTF-R S628D; (b) DSR-S and dextranase, co-immobilized (Erhardt et al. 2008a); (c) DSR-S (Jördening et al. 2008).

of process parameters (temperature, wash duration, solvents), Figure 6 clearly shows the benefits of using the GTF-R S628D enzyme system as a common principle and the consequent benefit of using low acceptor concentration.

Figure 7 displays the process efficiency (equation (8)) of three enzymatic biocatalysts at various sucrose/glucose concentrations. To compare all systems, batch operation with ISPR was assumed. The efficiency is an integral measure of the reaction and adsorption as well as for the specific load of zeolites. Its computation requires all kinetic models developed in the previous sections. For all systems the matrix depicts a single optimal process condition. Regarding the DSR-S system, the optimal sucrose/glucose concentration obtained from modeled data is in good agreement with the experimentally determined optimal process parameters (Ergezinger et al. 2006).

Optimal process parameters from Table II indicate that biocatalysts with a low affinity for glucosyl transfer (high K_Y) require high amounts of the acceptor glucose. Thus, the intuitive guess that a low K_Y (high molar yield coefficient, respectively) would allow for a lower glucose concentration in the reactor can be confirmed by computation. Furthermore, K_Y affects the maximum attainable process efficiency and a direct correlation between these two factors may be made. A 25-fold higher K_Y for the GTF-R variant than the DSR-S enzyme gives a 21-fold higher efficiency (likewise for the co-immobilizate; see last column of Table II).

In summary, Figure 7 and Table II clearly show the superiority of the new enzyme variant GTF-R S628D for the production of isomaltose in a FBR with ISPR. Also, process efficiency diagrams are a useful tool for the qualitative and quantitative assessment of different enzymatic systems for bioprocess development.

Conclusions

The GTF-R enzyme variant has been characterized physicochemically. The enzyme had long-term stability at pH 5.8 in acetate buffer at 30°C. Additionally, the enzyme variant possesses a K_M three times higher than the wild-type GTF-R, but a 5–25 times higher affinity for glucosyl transfer as compared with the DSR-S GTF ($K_{Y,GTF\text{-}R}$ = 0.8 mol mol^{-1}). A model was developed for combined computation of reaction kinetics and *in situ* product adsorption in a continuous reaction system. As a proof-of-concept for modeling and scale-up, a continuous FBR with ISPR was operated at semi-technical scale for 192 h. Further, a DSP scheme for zeolites was examined and product purities up to 90% could be obtained. Integral bioprocess modeling proved to be a powerful tool to assess the process efficiency of the GTF-R variant and two further GTFs for applications using ISPR. The superiority of the variant GTF-R S628D with its high selectivity could be demonstrated. Furthermore, the bioprocess model allowed for the identification of

Table II. Optimal process conditions and efficiencies for examined enzyme systems.

	Sucrose (mM)/glucose (mM)	Efficiency (mg g^{-1} h^{-1})	Product of efficiency and affinity K_Y (mg g^{-1} h^{-1}×mol mol^{-1})
GFT-R S628D	150/600	38.4	31
DSR-S + dextranase	260/900	8.4	36
DSR-S	200/1500	1.8	33

optimal process conditions for the three enzymatic systems.

Acknowledgements

This work is embedded in the collaborative research center SFB 578 'Development of biotechnological processes by integrating genetic and engineering methods – From gene to product'. The authors acknowledge the financial support provided by the German Research Foundation (DFG) and thank the collaborators (especially Dipl.-Biotechnol. Manuel Holtkamp for assistance with the reactor set-up) for their combined efforts and helpful discussions. We are very thankful to Wolfgang Grassl and Prof. Siegmund Lang (both of the Institute of Biochemistry and Biotechnology, TU Braunschweig) for placing fermentation equipment at our disposal.

References

Berensmeier S. 2003. Two different approaches for enzymatic carbohydrate synthesis: β-Elimination from polysaccharides by pectate lyase and oligosaccharide synthesis by glucosyltransferases. Braunschweig (Ger): Technical University Braunschweig. pp. 133.

Berensmeier S, Buchholz K. 2004. Separation of isomaltose from high sugar concentrated enzyme reaction mixture by dealuminated-zeolite. Separ Purif Technol 38:129–138.

Berensmeier S, Ergezinger M, Bohnet M, Buchholz K. 2004. Design of immobilised dextransucrase for fluidised bed application. J Biotechnol 114:255–267.

Berensmeier S, Jördening H, Buchholz K. 2006. Isomaltose formation by free and immobilized dextransucrase. Biocatal Biotransformation 24:280–290.

Buchholz K, Seibel J. 2003. In: Eggleston G, Côté GL, editors. Oligosaccharides in food and agriculture. Washington, DC: American Chemical Society. pp. 63–74.

Dols M, Remaud-Simeon M, Willemot R, Demuth B, Jördening H, Buchholz K, Monsan P. 1999. Kinetic modeling of oligosaccharide synthesis catalyzed by *Leuconostoc mesenteroides* NRRL B-1299 dextransucrase. Biotechnol Bioeng 63:308–315.

Ergezinger M. 2006. Integrierte enzymatische Produktion und Adsorption von Isomaltose in einem Mehrphasenreaktor. Braunschweig (Ger): Technical University Braunschweig. pp. 124.

Ergezinger M, Bohnet M, Berensmeier S, Bucholz K. 2006. Integrated enzymatic synthesis and adsorption of isomaltose in a multiphase fluidized bed reactor. Eng Life Sci 6.

Erhardt F, Kügler J, Chakravarthula R, Jördening H. 2008a. Co-immobilization of dextransucrase and dextranase for the facilitated synthesis of isomalto-oligosaccharides: preparation, characterization and modeling. Biotechnol Bioeng 100: 673–683.

Erhardt F, Stammen S, Jördening H. 2008b. Production, characterization and (co-) immobilization of dextranase from *Penicillium aculeatum*. Biotechnol Lett 30:1069–1073.

Goulas A, Cooper J, Grandison A, Rastall R. 2004. Synthesis of isomaltooligosaccharides and oligodextrans in a recycle membrane bioreactor by the combined use of dextransucrase and dextranase. Biotechnol Bioeng 88:778–787.

Hansson T, Adlercreutz P. 2001. Optimization of galactooligosaccharide production from lactose using β-glycosidases from hyperthermophiles. Food Biotechnol 15:79–97.

Heerze L, Armstrong G. 2002. Treatment of *C. difficile* toxin B associated conditions. United States Patent 6465435. Google Patents.

Heincke K, Demuth B, Jördening H, Buchholz K. 1999. Kinetics of the dextransucrase acceptor reaction with maltose – experimental results and modeling. Enzyme Microb Technol 24:523–534.

Hellmuth H, Wittrock S, Kralj S, Dijkhuizen L, Hofer B, Seibel J. 2008. Engineering the glucansucrase GTFR enzyme reaction and glycosidic bond specificity: toward tailor-made polymer and oligosaccharide products. Biochemistry 47:6678–6684.

Hilker I, Alphand V, Wohlgemuth R, Furstoss R. 2004. Microbial transformations, 56. Preparative scale asymmetric Baeyer–Villiger oxidation using a highly productive 'two-in-one' resin-based *in situ* SFPR concept. Adv Synth Catal 346:203–214

Holtkamp M, Erhardt F, Jördening H, Scholl S. 2009. Reaction-integrated separation of isomaltose by ad- and desorption on zeolite. Chem Eng Process 48:852–858.

Jördening H, Erhardt F, Holtkamp M, Buchholz K, Scholl S. 2008. Verfahrens- und Katalysatordesign als Aufarbeitungsstrategie für die enzymatische Darstellung von Isomaltose. Chem Ing Tech 80:867–874.

Kannagi R, Izawa M, Koike T, Miyazaki K, Kimura N. 2004. Carbohydrate-mediated cell adhesion in cancer metastasis and angiogenesis. Cancer Sci 95:377–384.

Kim D, Day D. 1994. A new process for the production of clinical dextran by mixed-culture fermentation of *Lipomyces starkeyi* and *Leuconostoc mesenteroides*. Enzyme Microb Technol 16: 844–848.

Koepsell H, Tsuchiya H, Hellman N, Kazenko A, Hoffman C, Sharpe E, Jackson R. 1953. Enzymatic synthesis of dextran acceptor specificity and chain initiation. J Biol Chem 200: 793–801.

Kralj S, van Geel-Schutten I, Faber E, van der Maarel M, Dijkhuizen L. 2005. Rational transformation of *Lactobacillus reuteri* 121 reuteransucrase into a dextransucrase. Biochemistry 44:9206–9216.

Kubik C, Sikora B, Bielecki S. 2004. Immobilization of dextransucrase and its use with soluble dextranase for glucooligosaccharides synthesis. Enzyme Microb Technol 34:555–560.

Landsteiner K. 2004. Uber Agglutinationserscheinungen Normalen Menschlichen Blutes (On agglutination phenomena of normal human blood). Landmarks in Medical Genetics: Classic Papers with Commentaries, Oxford University Press, USA, pp. 112.

Miller A, Robyt J. 1986. Inhibition of dextransucrase by Zn^{2+}, Ni^{2+}, Co^{2+}, and tris(hydroxymethyl)aminomethane (Tris). Arch Biochem Biophys 248:579–586.

Monchois V, Reverte A, Remaud-Simeon M, Monsan P, Willemot R. 1998. Effect of *Leuconostoc mesenteroides* NRRL B-512F dextransucrase carboxy-terminal deletions on dextran and oligosaccharide synthesis. Appl Environ Microbiol 64: 1644–1649.

Monsan P, Paul F. 1995. Enzymatic synthesis of oligosaccharides. FEMS Microbiol Rev 16:187–192.

Moulis C, Joucla G, Harrison D, Fabre E, Potocki-Veronese G, Monsan P, Remaud-Simeon M. 2006. Understanding the polymerization mechanism of glycoside-hydrolase family 70 glucansucrases. J Biol Chem 281:31254–31267.

Mountzouris K, Gilmour S, Rastall R. 2002. Continuous production of oligodextrans via controlled hydrolysis of dextran in an enzyme membrane reactor. J Food Sci 67:1767–1771.

Naessens M, Cerdobbel A, Soetaert W, Vandamme E. 2005. *Leuconostoc* dextransucrase and dextran: production, properties and applications. J Chem Technol Biotechnol 80:845–860.

Nilsson U, Heerze L, Liu Y, Armstrong G, Palcic M, Hindsgaul O. 1997. Immobilization of reducing sugars as toxin binding agents. Bioconjugate Chem 8:466–471.

Pereira A, Costa F, Rodrigues M, Maugeri F. 1998. *In vitro* synthesis of oligosaccharides by acceptor reaction of dextransucrase from *Leuconostoc mesenteroides*. Biotechnol Lett 20:397–401.

Pijning T, Vujicic-Zagar A, Kralj S, Eeuwema W, Dijkhuizen L, Dijkstra B. 2008. Biochemical and crystallographic characterization of a glucansucrase from *Lactobacillus reuteri* 180. Biocatal Biotransformation 26:12–17.

Roberfroid M. 2007. Prebiotics: the concept revisited. J Nutr 137:830S–837S.

Robyt J, Eklund S. 1983. Relative, quantitative effects of acceptors in the reaction of *Leuconostoc mesenteroides* B-512F dextransucrase. Carbohydr Res 121:279–286.

Schiweck H, Munir M, Rapp K, Schneider B, Vogel M. 1990. Use of sucrose as an industrial bulk chemical and production of isomaltulose and isomalt. Zuckerind (Berl) 115:555–565.

Seeberger P, Werz D. 2007. Synthesis and medical applications of oligosaccharides. Nature 446:1046–1051.

This paper was first published as an Early Online Article on 8 December 2009.

Sumner J, Howell S. 1935. A method for determination of invertase activity. J Biol Chem 108:1–54.

Taguchi H, Sasatani K, Nishitani H, Okumura K. 1997. Finding of UDP-glucose:nicotinic acid-*N*-glucosyltransferase activity in cultured tobacco cells and its properties. Biosci Biotechnol Biochem 61:720–722.

Taniguchi H. 2004. Carbohydrate research and industry in Japan and the Japanese Society of Applied Glycoscience. Starch-Stärke 56:1–5.

Tanriseven A, Dogan S. 2002. Production of isomalto-oligosaccharides using dextransucrase immobilized in alginate fibres. Process Biochem 37:1111–1115.

Tuomanen E, Fujiwara T, Hoshino T, Ooshima T, Sobue S, Hamada S. 2000. Purification, characterization, and molecular analysis of the gene encoding glucosyltransferase from *Streptococcus oralis*. Infect Immun 68:2475–2483.

Vetere A, Gamini A, Campa C, Paoletti S. 2000. Regiospecific transglycolytic synthesis and structural characterization of 6-*O*-α-glucopyranosyl-glucopyranose (isomaltose). Biochem Biophys Res Commun 274:99–104.